Seasonal variations of the upper ocean in the Scotia Sea and West of the Antarctic Peninsula as measured from instrumented seals

Alex Ruiz Urbaneja

Curso 2021/2022

Tutores:

Miguel Borja Aguiar González

Mª de los Ángeles Marrero Díaz

Trabajo Fin de Título para la obtención del título de Ciencias del Mar

Título:

Seasonal variations of the upper ocean in the Scotia Sea and West of the Antarctic Peninsula as measured from instrumented seals.

Datos personales:

Nombre: Alex

Apellidos: Ruiz Urbaneja

Titulación: Grado en Ciencias del Mar

Datos del trabajo:

Tutor: Miguel Borja Aguiar González

Tutor: Mª de los Ángeles Marrero Díaz

Empresa: Grupo de Oceanografía Física Y Geofísica Aplicada (OFYGA).

Departamento: Departamento de Física. Universidad de Las Palmas de Gran Canaria.

Firmas:

Estudiante: **Tutor**: **Cotutor**:

Fecha: 1 de julio de 2022.

INDEX

1 INTRODUCTON 5
1.1 BRANSFIELD STRAIT AND THE CENTRAL WEST ANTARCTIC PENINSULA 7
1.2 THE SCOTIA SEA 9
1.3 OBJECTIVES 9
2 DATA AND METHODS 10
2.1. MONITORING SYSTEM 11
2.2. DATA PROCESSING 13
3 RESULTS 14
3.1. SELECTION OF INSTRUMENTED SEALS 14
3.1.1. SURFACE DISTRIBUTION OF TEMPERATURE 15
3.1.3. *SURFACE AND SUBSURFACE DISTRIBUTION OF TEMPERATURE IN THE SCOTIA SEA* 18
4 DISCUSSIONS 25
5 CONCLUSIONS 25
6 REFERENCE 26

ACRONYMS LIST:

AASW. Antarctic Surface Water
ACC. Antarctic Circumpolar Current
AP. Antarctic Peninsula
BC. Bransfield Current
CC. Antarctic Coastal Current
CDW. Circumpolar Deep Water
CLS. *Collecte Localisation Satellites*
CWAP. Central West Antarctic Peninsula
LCDW. Lower Circumpolar Deep Water
mCDW. modified Circumpolar Deep Water
MEOP. Marine Mammals Exploring the Oceans Pole to Pole
PF. Peninsula Front
SSI. South Shetland Islands
TBW. Transitional Zonal Water with Bellingshausen Sea influence
TWW. Transitional Zonal Water with Weddell Sea influence
UCDW. Upper Circumpolar Deep Water
WW. Winter Water

Acknowledgements:

The first author is grateful to the *Ministerio de Educación y Formación Profesional* for the financial support provided through the grant 22AE/0796465.

I would also like to thank my tutors, Miguel Borja Aguiar González and Mª de los Ángeles Marrero Díaz and department colleagues.

Abstract:

In the Southern Ocean, the Scotia Sea and Bransfield Strait represent two major exits through which water masses driven by the western boundary current system of the Weddell Sea gyre leave the basin and feed the global thermohaline circulation. Furthermore, the South Shetland Islands and the Antarctic Peninsula (AP) are the locations where the relatively warm and strong Antarctic Circumpolar Current (ACC) flows closest to Antarctica, where some of the largest freshwater reservoirs on the planet can be found. However, due to the local hazardous weather conditions and sea-ice coverage that prevail through the fall and winter seasons, a year-round description of the regional hydrography has been traditionally hampered, especially in areas shallower than 1000 m where the standard parking depth of the freely drifting Argo floats prevent them to enter. The year-round hydrography of these shallower areas, with a greater influence in coastal scenarios, is of key interest given the role that the ocean plays as a thermal forcing to glacier retreat in polar regions.

In the upper ocean of the study area (0-400 m), five water masses govern the hydrography: Antarctic Surface Water (AASW), Winter Water (WW), Transitional Zonal Water with Bellingshausen Sea influence (TBW), Transitional Zonal Water with Weddell Sea influence (TWW) and modified Circumpolar Deep Water (mCDW). To characterize the seasonal variations these water masses may experience, we use a set of historical data based on observations from instrumented seals. These seals migrate every year, during the warm seasons, from the South Georgia Island and South Orkney Islands towards the south along the west Antarctic Peninsula, performing the reverse route as the colder seasons evolve.

Available observations enable the construction of a series of transects of temperature and salinity down to 400 m depth, which cover the year-round variability of the regional hydrography. These transects extend over 2000 km, sampled during for almost two months. Notably, on two occasions, the seals remained over nearly the same area in the Scotia Sea for several months, acting like a ‘living mooring’ and recording the time-varying temperature and salinity properties of local water masses through different seasons.

Results in this study show the temperature and salinity variations governing the seasonal water mass transformation of the upper ocean in the Scotia Sea and West Antarctic Peninsula.

1 INTRODUCTON

Antarctica is one of the harshest and most extreme regions on the planet due to its low temperatures and its constant transformation by the formation and melting of its territory.

The region of study in this work spans over the Scotia and Bellingshausen seas (Figure 1), connecting the South Georgia Island (54°S, 36°W) and the Central West Antarctic Peninsula (CWAP), running along the oceanward side of the South Shetland Islands (SSI).

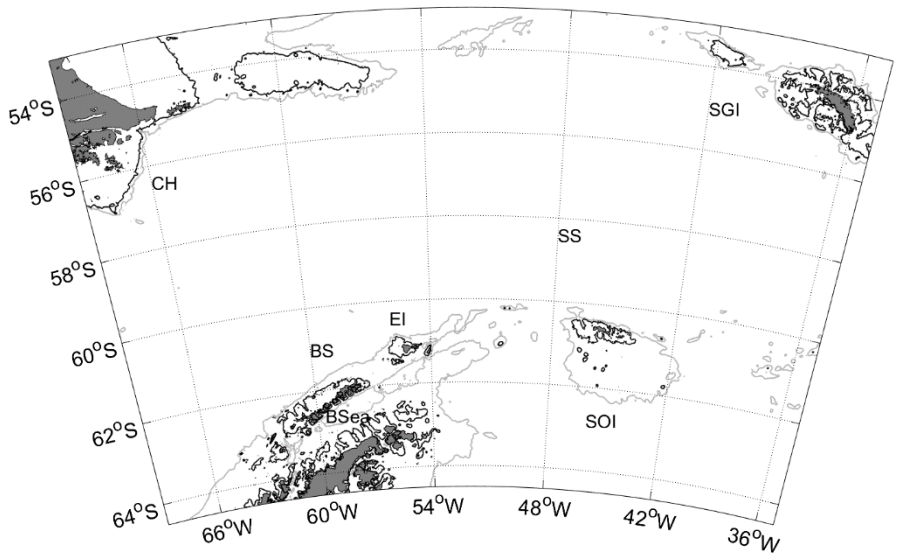

Figure 1: Region of study with indication to major geographical features. Acronyms stand for: Brasnfield Strait (BS), Elephant Island (EI), South Georgia (SGI), South Orkney Island (SOI), Cape Horn (CH), Scotia Sea (SS), Bellingshausen Sea (BSea). The isobath of 200 m (1000 m) is highlighted in black (grey).

This region is of high scientific interest due to its oceanographic context. On the one hand, the Scotia Sea represents the main route for inter-basin exchange of Weddell Sea waters with the global thermohaline circulation *(Reeve et al., 2019; Naveira Garabato et al., 2002*). On the other hand, the SSI and the AP are the locations where the relatively warm and strong ACC flows closest to Antarctica, where some of the largest freshwater reservoirs on the planet can be found.

Especially intriguing is the seasonal hydrography governing the northern shelf of the SSI (Figure 2), a domain through which the Bransfield Current (BC) recirculates during summer driven by cross-shelf density gradients (*Sangrà et al., 2017*) which are of unknown existence during other seasons. The intriguing aspect lies on the fact that, without a year-round cross-shelf density gradient, the Bransfield Gravity Current should not be expected to recirculate given the strong and opposing westerlies forcing the upper ocean regionally.

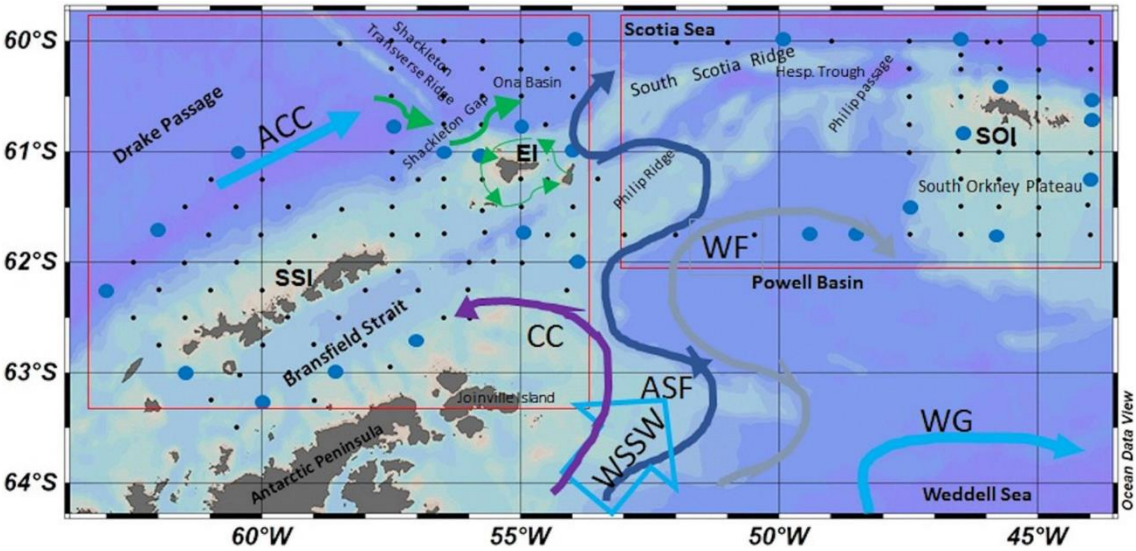

Figure 2: Sketch of the circulation in the Scotia Sea and northwestern Weddell Sea. The acronyms stand for: Antarctic Circumpolar Current (ACC), Antarctic Coastal Current (CC), Antarctic Slope Front (ASF), Weddell Front (WF), Weddell Gyre (WG), and Weddell Sea shelf water (WSSW)(Modified from Bizsel & Ardelan, 2007).

Due to the complexity of the ocean circulation in this region, where inter-basin exchanges of water masses occur, we describe below the major features characterizing its oceanography under two subdomains: (1) Bransfield Strait and the Central West Antarctic Peninsula; and (2) the Scotia Sea.

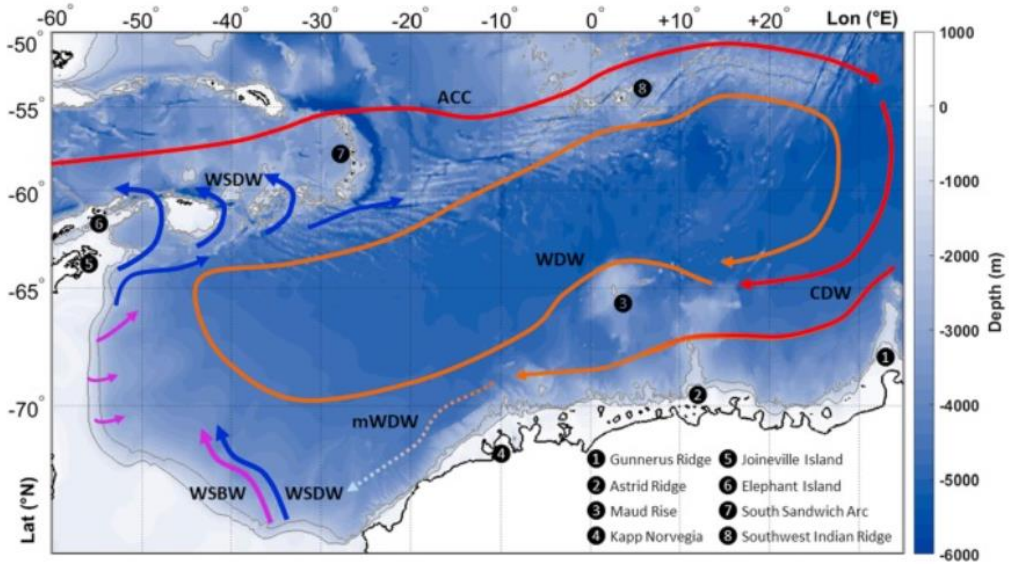

Figure 3: Current map of the Weddell Sea and the Bransfield Strait entrance.(From Reeve et al., 2019)

1.1 BRANSFIELD STRAIT AND THE CENTRAL WEST ANTARCTIC PENINSULA

The Bransfield Strait is in the Southern Ocean, between the South Shetland Islands and the Antarctic Peninsula, and represents a transitional zone between the water masses governing the Bellingshausen Sea, to the west, and the Weddell Sea, to the east *(García et al., 2002).*

The circulation and hydrography in BS is summarised in Figures 3 and 4, where two inflows stand *out (López et al., 1999; Sangrà et al., 2011; Sangrà et al., 2017, Veny et al., 2022)*: the eastward-flowing BC sourced from the Bellingshausen Sea, and the westward-flowing Antarctic Coastal Current (CC) sourced from the Weddell Sea. On the one hand, the BC transports TBW characterised by well-stratified, relatively warm (Θ > -0.4ºC) and fresh (<34.45) waters. On the other hand, the CC, which transports TWW, distinguished by homogeneous, colder (Θ < -0.4ºC) and saltier (>34.45) waters *(Sangrà et al., 2017).* Both water masses encounter each other at the sea surface, forming the Peninsula Front *(PF; García et al., 1994; López et al., 1999*). At subsurface, a core mCDW flows hugging the island slope of the SSI. This signal of mCDW is particularly relevant for the oceanic forcing to glacial melting over the continental and island shelves of Antarctica (*Cook et al., 2016).*

On the opposite side of the thermal oceanic forcing driven by the relatively warm mCDW, one finds the cold inflow of Weddell Sea waters (TWW), flowing southwestward along the Antarctic Peninsula. To this regard, TWW has been recently shown to play a key

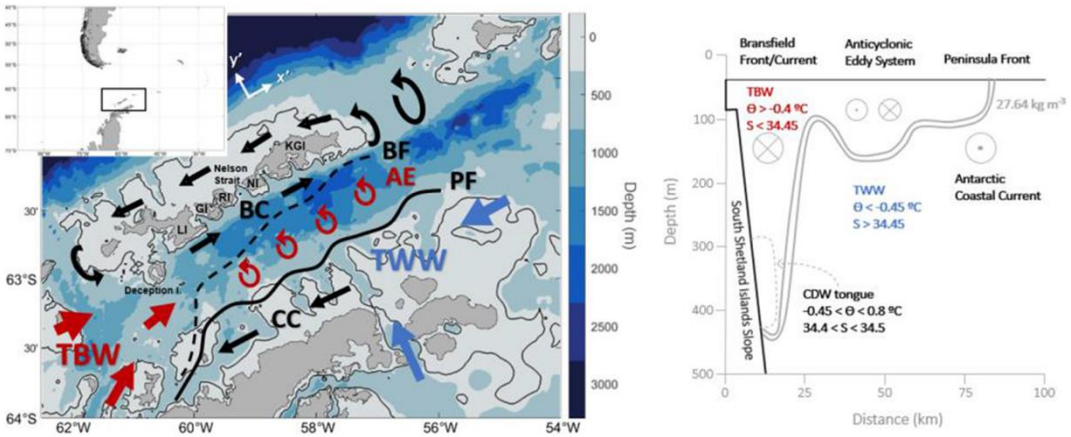

Figure 4: (a) Bathymetric map of the Bransfield Strait and summertime circulation pattern of the Bransfield Current System as described in (*Sangrà et al. (2011, 2017).* Acronyms for SSI are LI (Livingston Island), GI (Greenwich Island), RI (Robert Island), NI (Nelson Island) and KGI (King George Island). The isobath of 200 m is highlighted with a black contour. Acronyms for major features follow: AE (Anticyclonic Eddy), BC (Bransfield Current), BF (Bransfield Front), CC (Antarctic Coastal Current), PF (Peninsula Front), TBW (Transitional Bellingshausen Water), TWW (Transitional Weddell Water). (b) Sketch of the main components of the Bransfield Current System along a vertical section crossing the strait and the location of TBW (red) and TWW (blue). The Circumpolar Deep Water (CDW, black) tongue is distinguished by its temperature which is relatively higher than the surrounding waters *(From Veny et al., 2022).*

rolein maintaining and/or slowing down the melting rates of glaciers around the northern Antartctic Peninsula *(Cook et al., 2016).*

Further south of the Bransfield Strait, the Central West Antarctic Peninsula is characterized by three water masses which typically appear in the TS diagrams following a v-shape (Figure 5). At surface, the thermohaline structure is exposed to seasonally changing air-sea interactions, advection, formation and melting of sea-ice, wind mixing and the development/decay of upper water column stratification *(Gordon and Huber, 1984; Hofmann et al., 1996; Park et al., 1998; Smith et al., 1999).* These processes contribute to the large seasonal and spatial variations characterizing the AASW in the upper 100-150 m of the CWAP shelf and adjacent ocean.

During summertime, ASSW is then characterized by a scatter cluster of potential temperatures ranging from -1.8º to 1ºC and salinities of 33.0 to about 33.8 at σ< 27.1 kg m^{-3}. From fall to winter, the major seasonal change is the cooling and homogenization of the upper water column reducing the wide range of AASW variability. During winter, the end member of the AASW is formed, namely Winter Water (WW). WW is evident in summertime vertical sections as a distinct subsurface temperature minimum between -1.8º and -1ºC at salinities 33.8-34 and σ of 27.1-27.3 kg m^{-3} (depths about 150~m) *(Klinck et al., 2004).*

Off the shelf-break of the CWAP, the large-scale surface circulation (Figure 2) shows the ACC flowing eastward. The closeness of the ACC to the AP permits the latter to pump warm (>1.5ºC) and salty (34.5-34.7) Circumpolar Deep Water (CDW) onto the shelf below the permanent pycnocline at about 150-200 m *(Orsi et al., 1995; Hofmann and Klinck, 1998; Smith et al., 1999; Prezelin et al., 2000).* This occurs at specific sites where the entrance of CDW is allowed by the bathymetry such as in Marguerite Trough *(Klinck et al., 2004; Moffat et al., 2009)*. However, the parameter space of the CDW broadens on its pathway across the shelf where colder and fresher versions of CDW lead to mCDW (Figure 5). Other distinctive members of CDW are: the Upper CDW (UCDW), characterized by a temperature maximum up to 2ºC at a potential density of 27.6 kg m^{-3}; and, the Lower CDW (LCDW), characterized by a salinity maximum of 34.74 at a potential density above 27.7 kg m^{-3} *(Klinck et al., 2004; Moffat et al., 2009).*

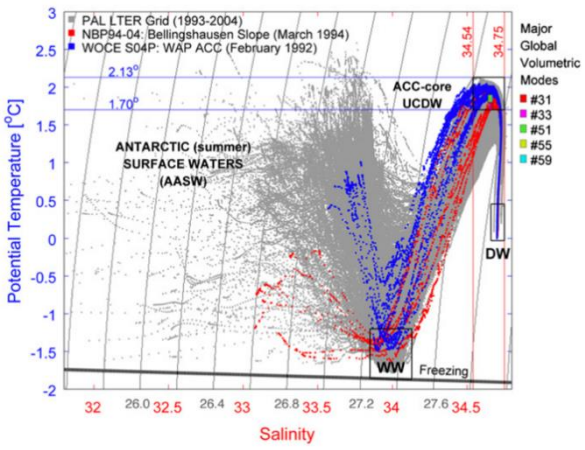

Figure 5. θ–S diagram for 12 years of summer PAL LTER CTD station data (grey). Key water masses, as they appear in the CWAP region, are indicated and labeled as follows: Upper Circumpolar Deep Water (UCDW); Winter Water (WW); Antarctic Surface Water (AASW) in summer; and a local ''end-member'' deep water: DW.

1.2 THE SCOTIA SEA

Over the Scotia Sea, the convergence of water masses from both the ACC and the Weddell Gyre occurs (Figure 2). In the upper ocean (0-400 m) of this area, the main water masses are AASW and WW in the first 300 m, followed by CDW and its modified versions of UCDW and LCDW at depths generally greater than 300 m depth *(Alberto C. Naveira Garabato et al., 2003; Palmer et al., 2012; R. Yu. Tarakanov, 2008).* Additionally, waters from the Weddell Sea are found leaking through the Scotia Sea towards the South Atlantic Ocean, and through Bransfield Strait towards the Central West Antarctic Peninsula driven by the CC (*Sangrà et al., 2011; Gertrud et al., 2016)*. The latter water mass is referred in the literature as TWW, introduced previously when describing major water masses in Bransfield Strait. In Figure 6, the TS parameter space for AASW, WW and CDW in the upper ocean of the Scotia Sea is presented as reported from historical databases in Patterson and Sievers (1980) for the transect named section II.

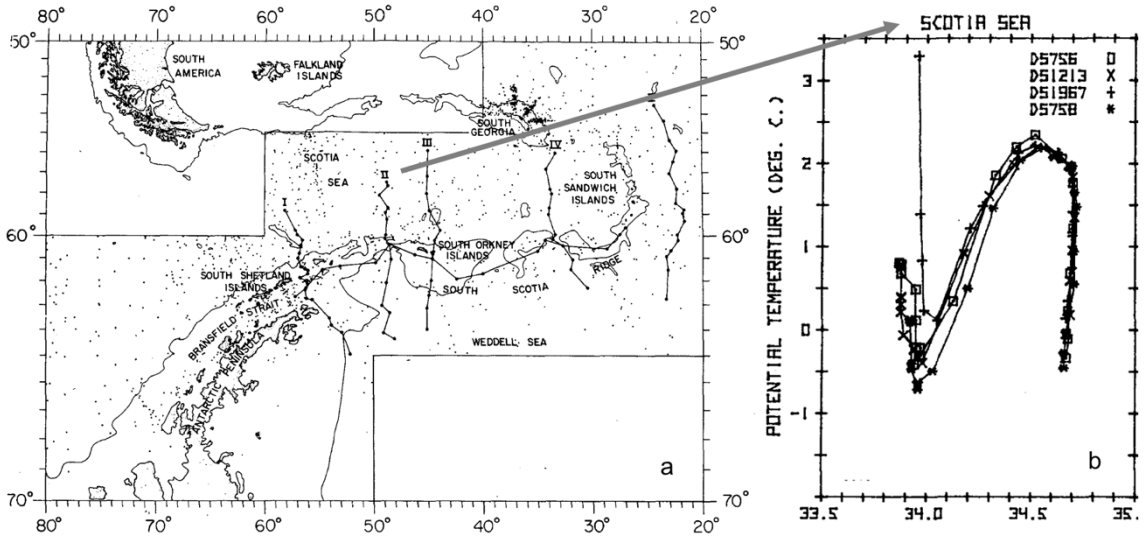

Figure 6: (a) Map with the distribution of historical hydrographic stations considered in Patterson and Sievers (1980). (b) TS diagram for stations along the section II in panel a (From Patterson and Sievers, 1980).

1.3 OBJECTIVES

Due to the local hazardous weather conditions and sea-ice coverage that prevail through the fall and winter seasons in polar regions, a year-round description of the regional hydrography in our area of study has been traditionally hampered. This is further complicated in areas shallower than 1000 m where the standard parking depth of the freely drifting Argo floats prevent them to enter. The year-round hydrography of these shallower areas, with a greater influence in coastal scenarios, is of key interest given the role that the ocean plays as a thermal forcing to glacier retreat in polar regions *(Cook et al., 2016).*

For the above reasons, we think the use of monitored mammals gives us a broader view of the region (seals are sampling the ocean continuously) without depending on the season, governing weather conditions, or bathymetry.

Accordingly, in this work we aim to characterize the seasonal variations of the upper ocean in the Scotia Sea and West of the Antarctic Peninsula using historical data from the MEOP project (*Marine Mammals Exploring the Oceans Pole to Pole;* see further details on the MEOP project in *Section 2*).

2 DATA AND METHODS

The MEOP project (*Marine Mammals Exploring the Oceans Pole to Pole*) project consists of an international collaboration for the study of polar regions with the use of monitored marine mammals. This project brings together several national programs to produce a quality-controlled comprehensive database of oceanographic data from each region, in addition to maintaining the current data portal from where information and oceanographic observations can be easily accessed. The countries that are part of the MEOP project are: Australia, Brazil, Canada, China, France, Germany, Norway, South-Africa, Swedan, UK, USA (further details on the MEOP project can be found at https://www.meop.net/).

The procedure of data collection is summarized in Figure 7. Every time the instrumented animal gets to the sea surface, the CTD (Conductivity-Temperature-Depth) data are transmitted via ARGOS communication to the center of data reception at the Collecte Localisation Satellites (CLS) Argos, Toulouse. Afterwards, a post-processing of the CTD data is performed *(Boehlert et al., 2001).* Lastly, the processed data are distributed to ocean data centers for open access to the scientific community. Further details about the monitoring system are provided in *Section 2.1*.

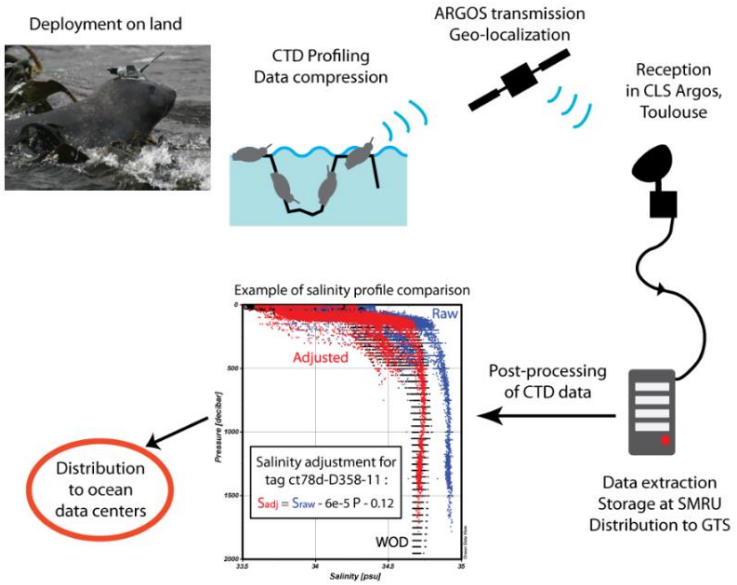

Figure 7: Scheme of data collection (From https://www.meop.net/).

Two examples of the CTD data which can be accessed from the MEOP project are provided in Figures 8 and 9. The identification codes for the instrumented animals generally follow as *ct-xx*, where xx stands for a given number that refers to a specific community. Then, each animal within a specific community is identified with a code such as *ct-xx-yy-zz*, where *yy* stands for a given animal and *zz* stands for the last two digits of the year. Thus, in Figure 8, the code *ct-39* refers to all observations collected by the

community 39; and, in Figure 9, the code *ct-39-40-08* refers to the animal 40 of that community in 2008.

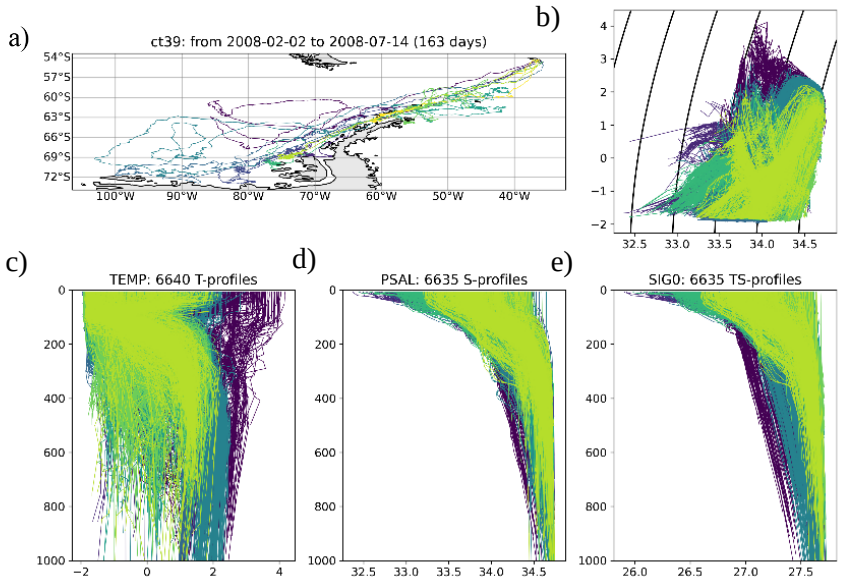

Figure 8: Map, vertical profiles and vertical sections provided by the MEOP project for the community of animals under the code ct-39. (a) Trajectory of the animal. (b) TS diagram. (c, d, e) Vertical profiles of temperature, salinity and density, respectively.

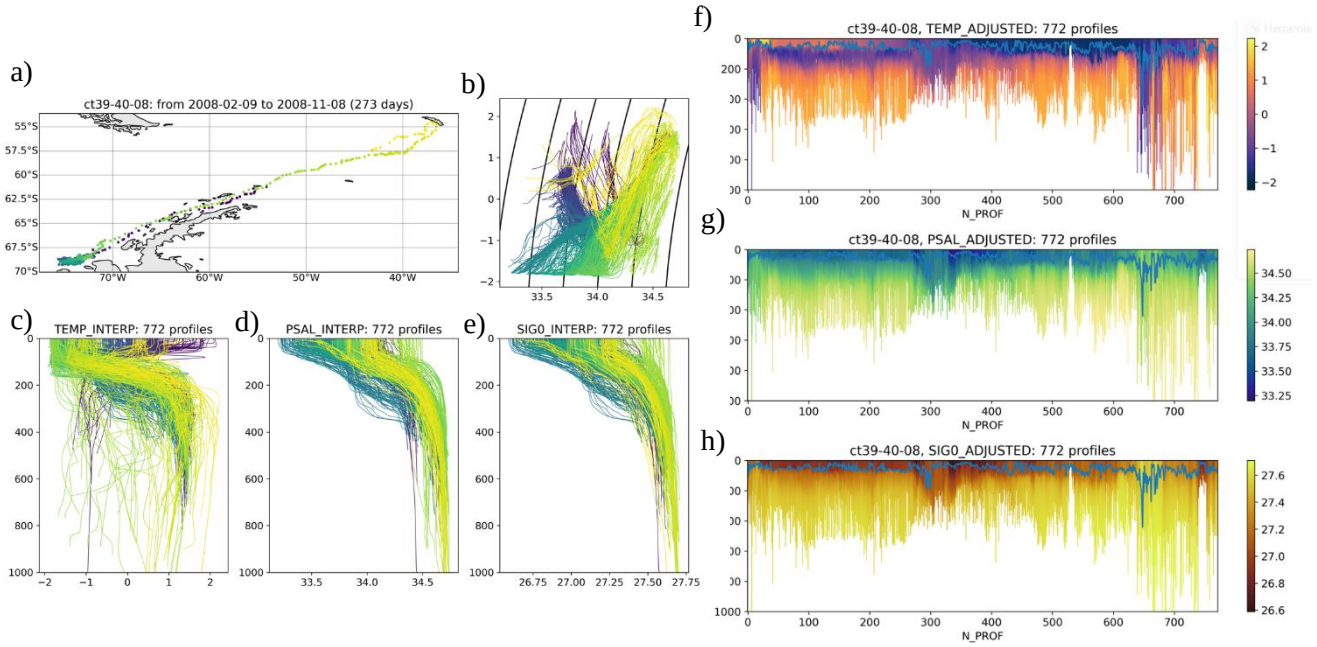

Figure 9: Map, vertical profiles and vertical sections provided by the MEOP project for the instrumented animal under the code ct-39-40-08. (a) Trajectory of the animal. (b) TS diagram. (c, d, e) Vertical profiles of temperature, salinity and density, respectively. (f, g, h) Vertical sections of temperature, salinity and density, respectively.

2.1. MONITORING SYSTEM

The device attached to the animal is a CTD-SRLD (Figure 10), developed by the Sea Mammal Research Unit of the University of St Andrews (Scotland) in cooperation with Valeport Ltd. *(Boehme et al., 2009).* The CTD tag has an algorithm which detects the deepest immersion point of the animal, and it starts gathering data about temperature, conductivity, and pressure until it gets to the surface. Then, the data are stored and, at the surface, are transmitted via the ARGOS satellite system to the data center, where the Sea Mammal Research Unit (SMRU) process the data*(Vincent et al., 2002)*.

The location of the animal at the end of the dive, where data are being collected, is estimated using a least squares method. A velocity filter is then applied to discard locations where the velocity should be too high to reach. Once the filter is applied, a linear interpolation is made between the locations that passed the filter. The accuracy is ±5 km *(Boehlert et al., 2001; Vincent et al., 2002).*

Importantly, the CTD tag is respectful with the animal and also have 0 impact on its life. Aiming that, the device must not weight more than the 2-5% of the animal total weight. The dimensions are 12 cm long, 7.2 cm wide and 6 cm height, plus 15 cm long of the antenna. *(Boehme et al., 2009).* The total volume is of 254 cm^3 with a total mass of 545±5 g in air and 255±5 g in sea water *(Boehme et al., 2009).*

Given that small changes in temperature and salinity are key, specially in polar regions, the error from the device being used should not be large. The CTD tag is accurate to ±0.01◦C and ±0.02, respectively. On the other hand, the pressure range provided by the manufacturer is up to 2000 dbar with an accuracy of better than 1 % of the full scale reading *(Boehme et al., 2009).*

Figure 10: CTD-Satellite Relay Data Logger (CTD-SRDL) with antenna (1), temperature sensor (2), inductive cell (3), pressure sensor (4), battery (5), communication port (6) and wet-dry sensor (7) (Boehme et al., 2009).

2.2. DATA PROCESSING

To characterize the seasonal variations of the upper ocean in the Scotia Sea and West of the Antarctic Peninsula, a set of observations collected by instrumented animals is analyzed and discussed in *Sections 3 and 4*.

The selection of the animals used in this study follows visual inspection of all available data from a total of 1564 instrumented animals. The first criterium to select a given animal responds to the trajectory they followed. Thus, after a first inspection, all animals which dived through the region of interest were selected. At a second stage, the selection proceeded through the identification of those animals which performed stable trajectories from the Scotia Sea towards the CWAP, or vice versa. By stable trajectories we mean trajectories through which the animal did not dive in circles or stay for too long around a given position, given that these circumstances break the clarity and sinopticity of neighboring measurements. The latter criterium is crucial as it allows the construction of transects which capture the seasonal water mass transformations we aim. Lastly, we select for this work a representation of 60 animals which cover all the seasons. However, we must note that some other animals (not shown here) performing similar trajectories were also inspected to confirm robustness and recurrency of the results. Those results are not shown in the present study to avoid redundancy.

The selected animals belong observations collected by the following countries: Brazil, Germany, UK and USA. Generally speaking, for each of these countries there are between 2 to 5 communities with about 10 individuals each.

For the characterization of the water mass transformations experienced through seasons, we use in the following sections horizontal maps which show the selected transects performed by each animal, and the corresponding vertical sections of potential temperature, salinity and potential density. These analyses are complemented with TS diagrams. Spatial smoothing and interpolation were performed for each transect as shown in the example in Figure 11. The smoothing accounts only for the immediate profile at each side around a given middle profile, and for vertical cells of 5 m. The interpolation is based on sparse linear algebra and discretization of partial differential equations. Essentially, the PDE is solved to be consistent with the information supplied and original data are preserved *(D'Errico, 2022).*
At this point we also find relevant to note that a further data processing (beyond that applied by the SMRU unit) and visual inspection of each profile may be advisable for double-checking before scientific publication of this work in a peer-reviewed journal.

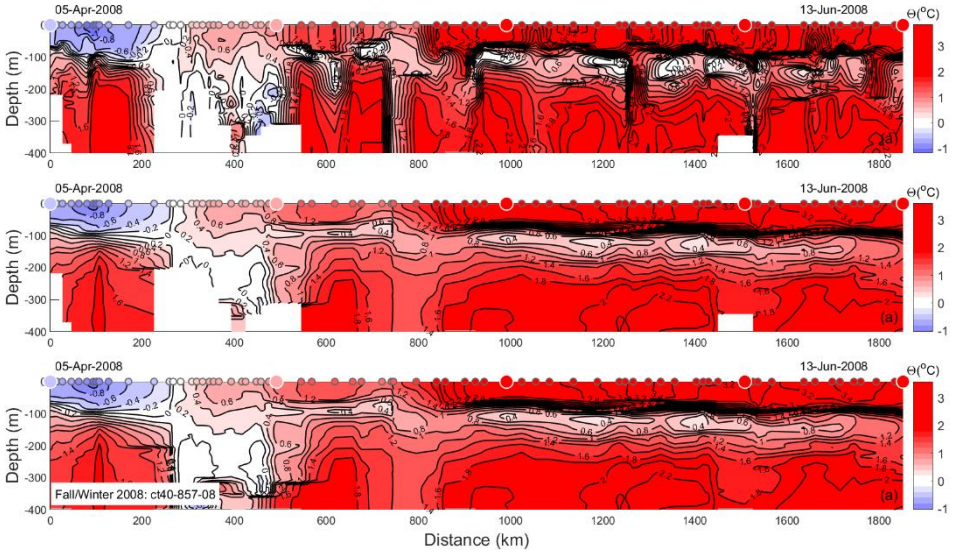

Figure 11: Vertical sections of potential temperature (ºC) as measured from the instrumented animalwith code ct40-857-08 in Winter/Spring. (a) Data as processed and delivered by the SMRU unit. (b) Data after spatial smoothing. (c) Data after interpolation.

3 RESULTS

The results are divided into the following subsections. In Section 3.1, we present the selection of instrumented seals used in this study, noting the main characteristics of the routes they followed. In Section 3.2, a set of vertical sections of ocean properties and TS diagrams are analysed aiming to describe the seasonal hydrography and water mass transformations occurring in the upper ocean of the study area. In Section 3.3, a selection of two instrumented seals which stayed in a reduced area of the Scotia Sea during several months is analysed.

For clarity, we define seasons in this work as follows: summer (December-January-February), fall (March-April-May), winter (June-July-August) and spring (September-October-November).

3.1. SELECTION OF INSTRUMENTED SEALS

Table 1 identifies the seven instrumented animals used in this study with indication to their identification (ID) code from the MEOP project, start and end dates (and locations), cumulative distance and mean diving speeds.

On average, these animals travelled at a diving speed about 84 km/day, with maximum speeds up to 120 km/day. This allowed performing transects as long as 2000 km long in about two months.

Id	Start date	End date	Start location		End location		Cumulative distance (km)	Diving speed (km/day)	Days
			Latitude (º)	Longitud (º)	Latitude (º)	Longitud (º)			
ct40-857-08	05-Apr-08	1-Jul-08	-64	-65	-55	-41	1852	80	87
ct37-780-08	30-Jun-08	1-Oct-08	-64	-66	-54	-37	2105	72	93
ct48-032-09	07-Sep-09	1-Oct-09	-64	-65	-54	-38	2054	106	24
ct48-041-09	27-Aug-09	25-Sep-09	-64	-67	-54	-38	2058	83	29
ct58-10971-09- down	28-Oct-09	11-Nov-09	-60	-51	-54	36	1360	110	14
ct58-10971-09- upload	19-Dec-09	04-Jan-10	-60	-51	-54	-37	1733	120	16
ct49-Tuborg-09	20-Feb-09	02-Dec-09	-55	-36	-54	-37	1209	50	285
ct40-Sheila-08	2-Feb-08	9-oct-08	-54	-37	-54	-37	1108	49	249

Table 1: List of instrumented seals used in this study. The main parameters characterizing the tracks are indicated.

Figures 12-14 present the tracks of the instrumented seals in Table 1 with colored markers, which show the temperature measured along their routes at 50 m (left-hand side panels) and 200 m (right-hand side panels) depth. From top to bottom, each row of panels shows the track of a given animal, where the corresponding ID is indicated in the legend.

Generally speaking, the instrumented animals in Figure 12 travelled from the eastern entrance of the Bransfield Strait towards South Georgia Island from October to November 2009, and from December 2009 to January 2010, respectively, thus capturing spring and summer seasons. The instrumented animals in Figure 13 travelled between South Georgia and West of the Antarctic Peninsula capturing, from top to bottom panels: fall to winter 2008, winter to spring 2008 and winter to spring 2009, respectively. Lastly, the instrumented animals in Figure 14 stayed through nearly the entire 2008 (panel a,b) and 2009 (panel c,d) diving around within a relatively reduced area in the Scotia Sea.

3.1.1. SURFACE DISTRIBUTION OF TEMPERATURE

Through spring and summer (Figure 12), the horizontal distributions of temperature near the surface (left-hand side panels for 50 m depth) suggest a combination of local atmospheric forcing and origin of source waters may be driving the observed spatial differences in the Scotia Sea. From south to north, the tracks show temperatures generally colder near the eastern entrance of BS than closer to South Georgia Island. This occurs during both seasons, though colder temperatures reach farther north during spring likely due to a cooler atmospheric is acting towards the north. See values around 0ºC (blue to red markers) as a reference to this feature. This pattern is also likely the response to a higher presence of cooler Weddell Sea waters (TWW) when closer to the eastern entrance of BS as compared to AASW governing the surroundings of South Georgia Island.

Evolving from fall to winter and spring (Figure 13), the horizontal distributions of temperature near the surface (left-hand side panels for 50 m depth) show a much more homogenous pattern along tracks from the West Antarctic Peninsula to the Scotia Sea,

suggesting the open ocean nature of these waters responds to AASW, cooling everywhere from fall to winter/spring.

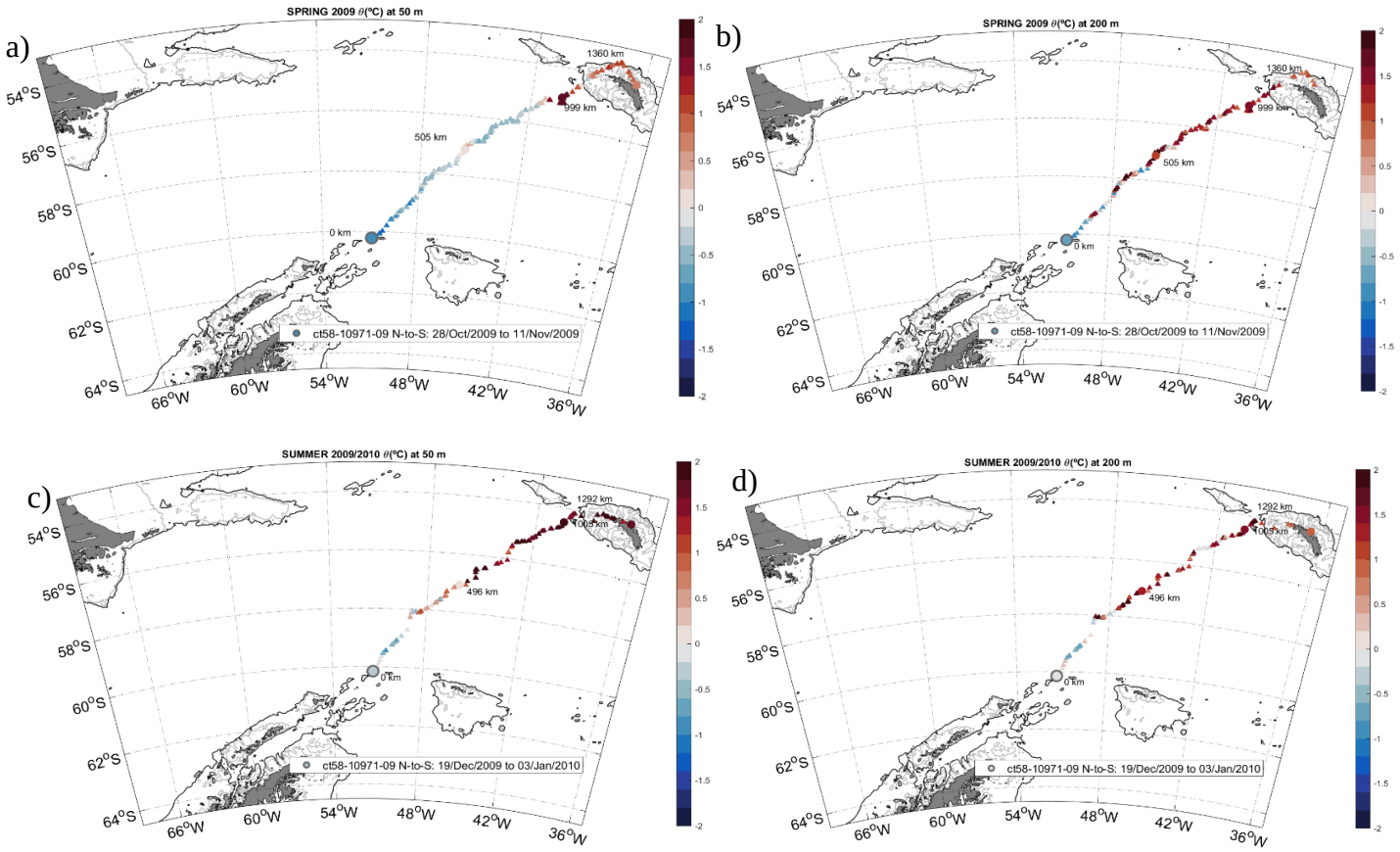

Figure 12: Springtime and summertime maps of the tracks followed by each of the instrumented seals of study: (a,b) ct58-10971-09; (c,d) ct58-10971-09. Colored markers show temperature at 50 m (left-hand side panels) and 200 m (right-hand side panels) depth. The seasons through which each animal collected measurements is indicated at the top of each panel.

3.1.2. SUBSURFACE DISTRIBUTION OF TEMPERATURE

Through all seasons in Figures 12 and 13, the horizontal distributions of temperature at subsurface (right-hand side panels for 200 m depth) suggest that no seasonal variability occurs in the Scotia Sea. Spatial differences are only observed when temperatures in the southern entrance of BS are compared to those closer to South Georgia Island (Figure 12). We attribute, the colder temperatures in the southern Scotia Sea are likely the signal of TWW carried by the leakage flows coming from the western boundary currents of the Weddell Sea. Differently, the warmer waters farther north in the Scotia Sea are likely governed by modified versions of CDW pumped from the ACC. This gradient seems to strengthen around 58ºS (isotherm of 0ºC) in the Scotia Sea.

For seals travelling farther south towards the West Antarctic Peninsula and along the northern side of the SSI (Figure 13, right-hand side panels), subsurface temperatures are also relatively warmer everywhere with no apparent seasonal variability, likely the signal

of offshore CDW pumped by the ACC. One exception occurs in Figure 13 b, when the instrumented seal crossed the island slope of the SSI and measured water masses over the northern island shelves, expected to be cooler than oceanward counterparts due to recirculated waters driven by the Bransfield Current around the SSI.

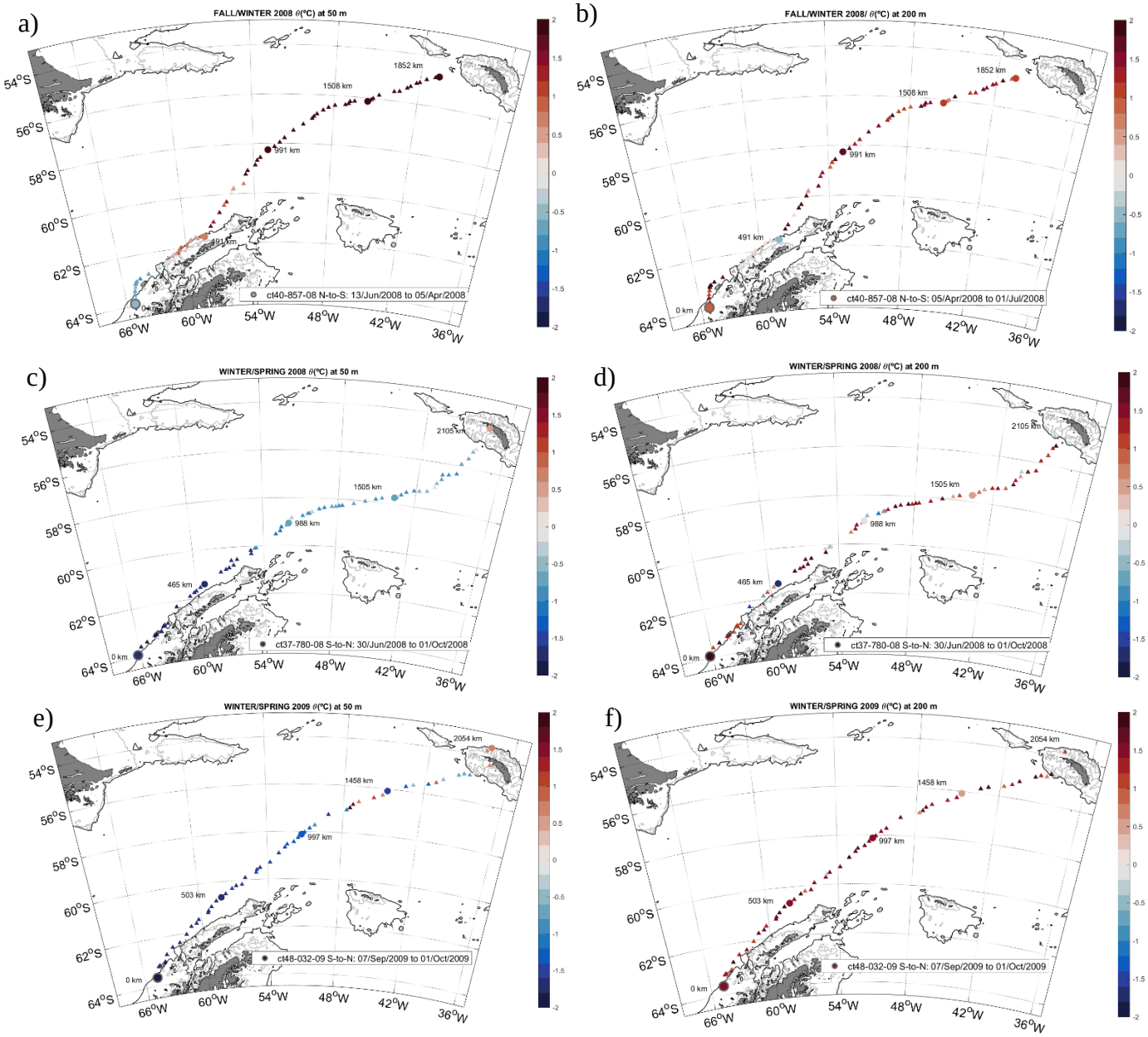

Figure 13: Fall, winter and springtime maps of the tracks followed by each of the instrumented seals of study: (a,b) ct40-857-08; (c,d) ct48-780-08; (e,f) ct37-032-09. Colored markers show temperature at 50 m (left-hand side panels) and 200 m (right-hand side panels) depth. The seasons through which each animal collected measurements is indicated at the top of each panel.

3.1.3. *SURFACE AND SUBSURFACE DISTRIBUTION OF TEMPERATURE IN THE SCOTIA SEA*

In Figure 14, the horizontal distributions of temperature near the surface (left-hand side panels for 50 m depth) and at subsurface (right-hand side panels for 200 m depth) support further than stronger seasonal variations (see extreme positive and negative values) occur at shallower levels as one could expect due their proximity to the ocean-atmosphere interface. At subsurface, where the atmospheric forcing is less prominent, spatial variations show generally colder (warmer) temperatures to the south (north) as a response to a higher influence of Weddell Sea waters (Circumpolar Deep Waters).

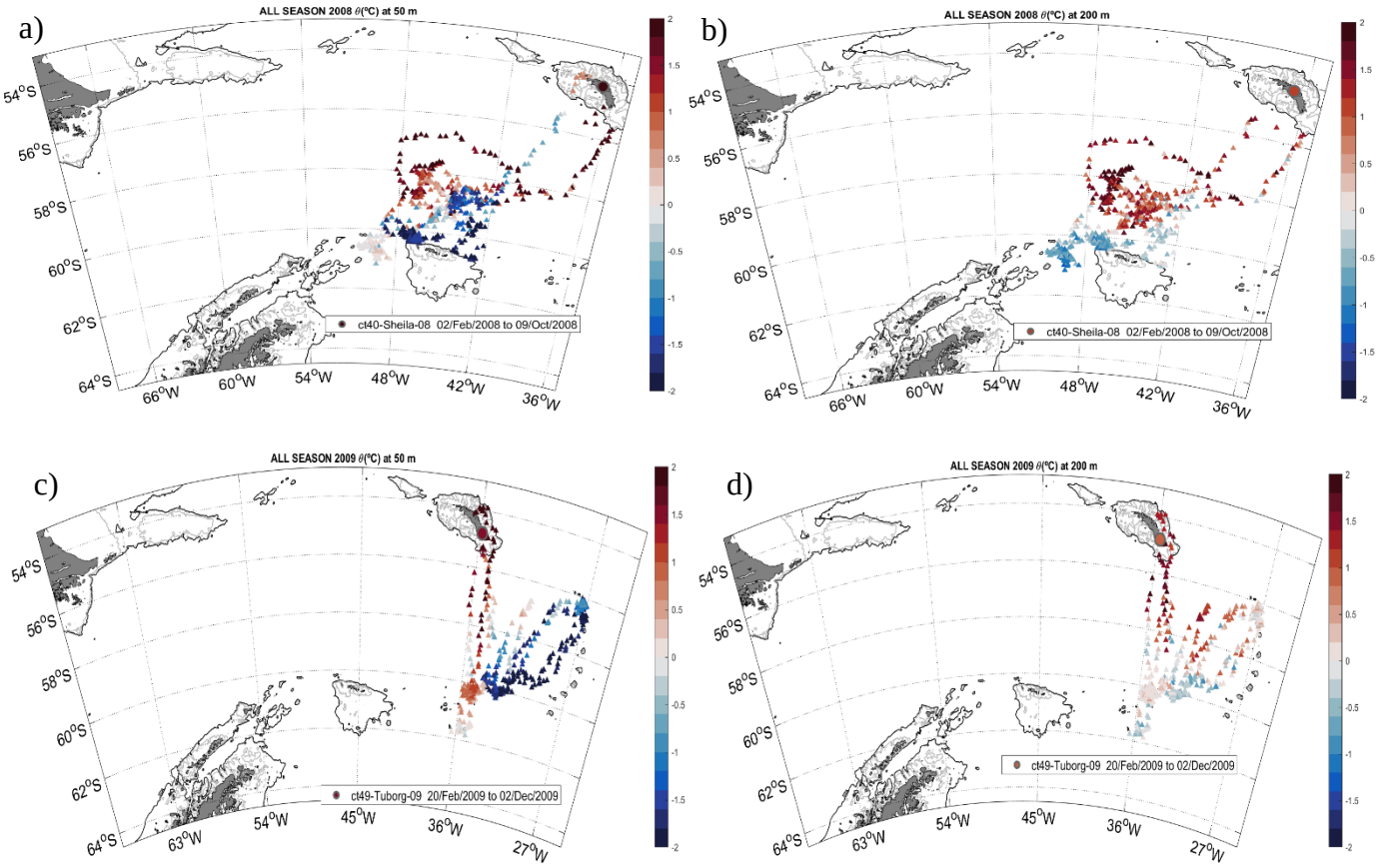

Figure 14: Maps of the time-varying temperature in the Scotia Sea as measured by the seals of study: (a) ct40-Sheila-08; (b) ct49-Tuborg-09. Colored markers show temperature at 50 m (left-hand side panels) and 200 m (right-hand side panels) depth. Each seal collected data through an entire year, 2008 and 2009, respectively (see the legend).

3.2.- SEASONAL HYDROGRAPHY AND WATER MASSES BETWEEN THE SCOTIA SEA AND WEST OF THE ANTARCTIC PENINSULA

3.2.1- SPRING AND SUMMER

Evolving through spring and summer, Figures 15 and 16 present the hydrography and major water masses in the Scotia Sea from the surface down to 400 m depth, following the tracks performed by the two instrumented animals in Figure 12 (panels *a,b* and *c,d*, respectively). Thus, the hydrographic structures In Figures 15 and 16 follow from the vertical sections of potential temperature, salinity and potential density (panels *a*, *b* and *c*). The water masses are analysed following the TS diagram in panel *d*. Subsequent seasons will be presented and analysed in an analogous fashion.

During springtime (Figure 15), the upper 100 m of the Scotia Sea presents cold surface waters (-1^o to 0^{o}C) near the eastern entrance of Bransfield Strait while warmer surface waters (0^o to 1.8^{o}C) prevail near South Georgia Island. Remarkably, this temperature gradient along the track strengthens around the isotherm of 0^{o}C (thermal front) at about 55.5^{o}S, before arrival to South Georgia Island. The colder surface waters are also slightly saltier near the eastern entrance of Bransfield Strait as opposed to near South Georgia Island. This pattern is likely the response to a higher presence of cooler Weddell Sea waters (TWW) when the seal dived closer to the eastern entrance of BS as compared to AASW governing the surroundings of South Georgia Island. Major water masses are identified and labelled in the TS diagram in Figure 15 *d* and *e*.

At subsurface, and close to the eastern entrance of Bransfield Strait, TWW extends vertically down to at least 400 m depth. A hundred kilometers away from that location, intrusions of warm CDW are evident rising from 400 m up to 100 m depth. Close to South Georgia Island, the warm pool of CDW (0^o to 2.2^{o}C) becomes prominent northward of the surface thermal front described above.

During summertime (Figure 16), the Scotia Sea presents an analogous hydrographic structure to that described for springtime with a key difference in the upper 100 m of the upper ocean: the atmospheric forcing has warmed up the surface ocean. Thus a WW layer becomes more prominent underlying warm AASW with a marked temperature minimum centred at 100 m depth at distances about 300 km away from the eastern entrance of BS and towards South Georgia Island. Near Bransfield Strait, TWW continues being dominant through the first 400 m. The subsurface warm pool of mCDW extends now from the domain where TWW ends towards South Georgia Island. These water masses are identified and labelled in the TS diagram in Figure 16 *d* and *e*.

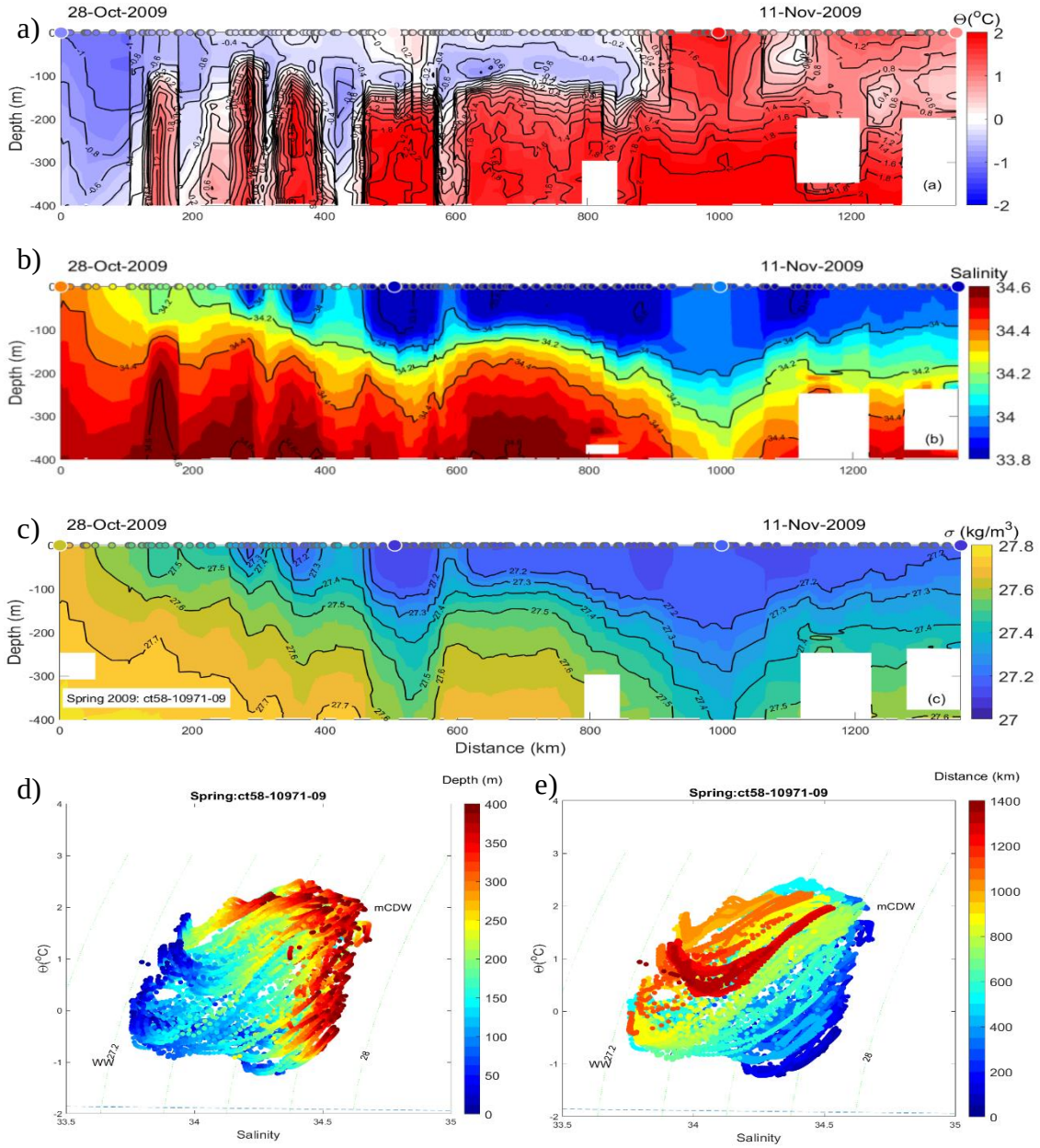

Figure 15: Springtime vertical sections of (a) potential temperature, (b) salinity and (c) potential density. TS diagrams with shades of colors showing (d) depth and (e) distance.

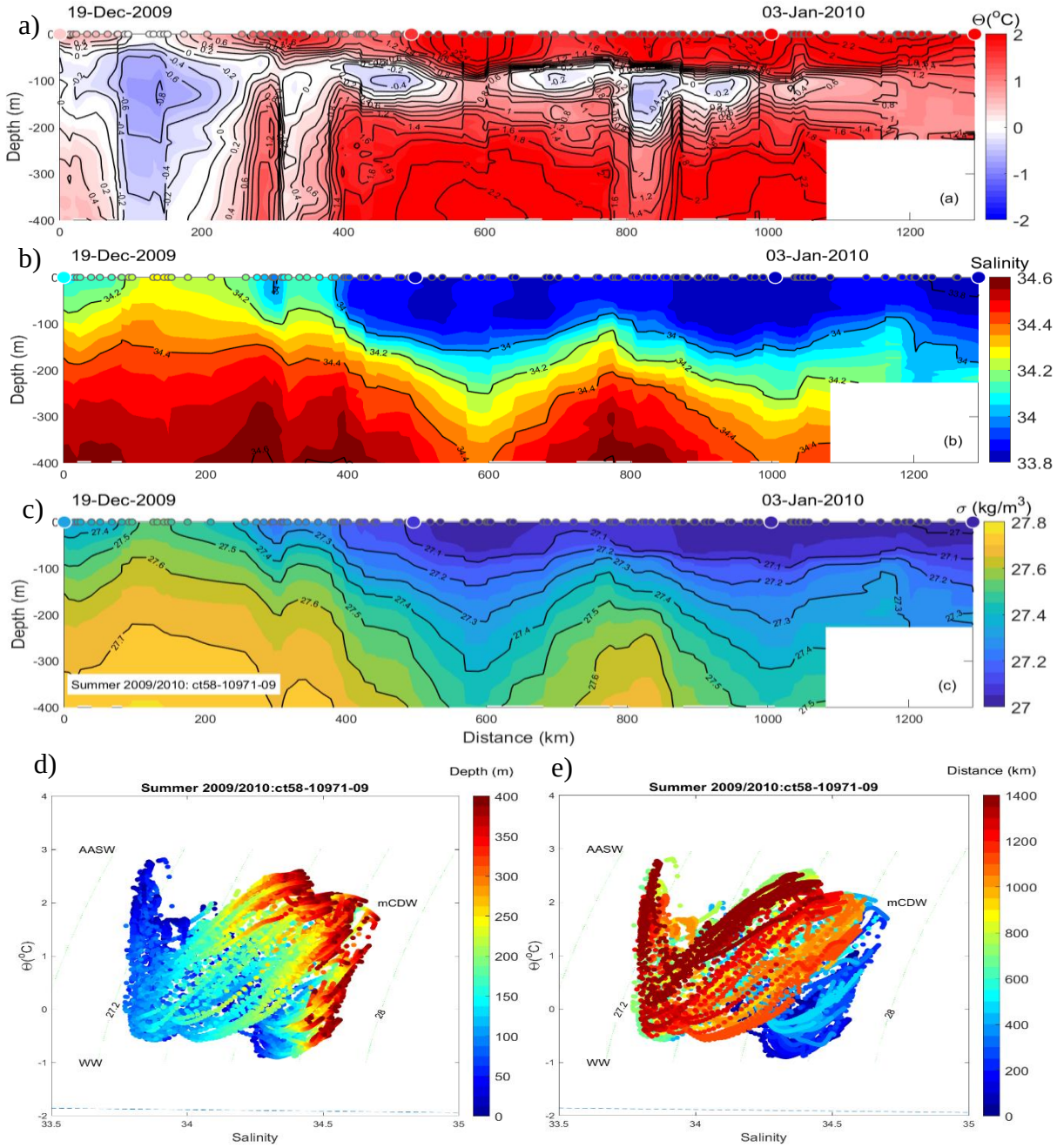

Figure 26: Summertime vertical sections of (a) potential temperature, (b) salinity and (c) potential density. TS diagrams with shades of colors showing (d) depth and (e) distance.

3.2.2- FALL, WINTER AND SPRING

Figures 17 and 18 present the hydrographic structure and water masses of the Scotia Sea and West of the Antarctic Peninsula through fall to spring from the tracks performed by the instrumented seals in Figure 13 (panels *a* to *d*).

Thus, the vertical sections in Figure 17 capture the fall/wintertime ocean properties of relatively warm AASW in the upper ocean, overlying a layer of WW (subsurface temperature minimum) and a deeper pool of warm and more saline mCDW. This is the case along the entire track except for the southernmost portion, where surface layers are

notably colder (-0.8ºC) than northward (up to 3.4ºC). This meridional gradient as the seasons evolve from fall to winter is the motivation behind the northward migration of the instrumented seal, looking for warmer temperatures to the north as the winter season advances more prominently in the south. Major water masses are identified and labelled in the TS diagram in Figure 17 *d* and *e*.

During wintertime (Figure 18), the most prominent feature is the cooling of the first 100 m of the water column down to near-freezing temperatures reaching -1.8ºC in the southernmost locations of the track. As the seal dived to the north, warmer surface temperatures are found due to the end of the winter season and start of spring. At subsurface, the entire domain is governed by a warm and saline pool of mCDW. Major water masses are identified and labelled in the TS diagram in Figure 17 *d* and *e*. This winter/springtime pattern was also captured by the seal with ID ct48-032-09 (see the

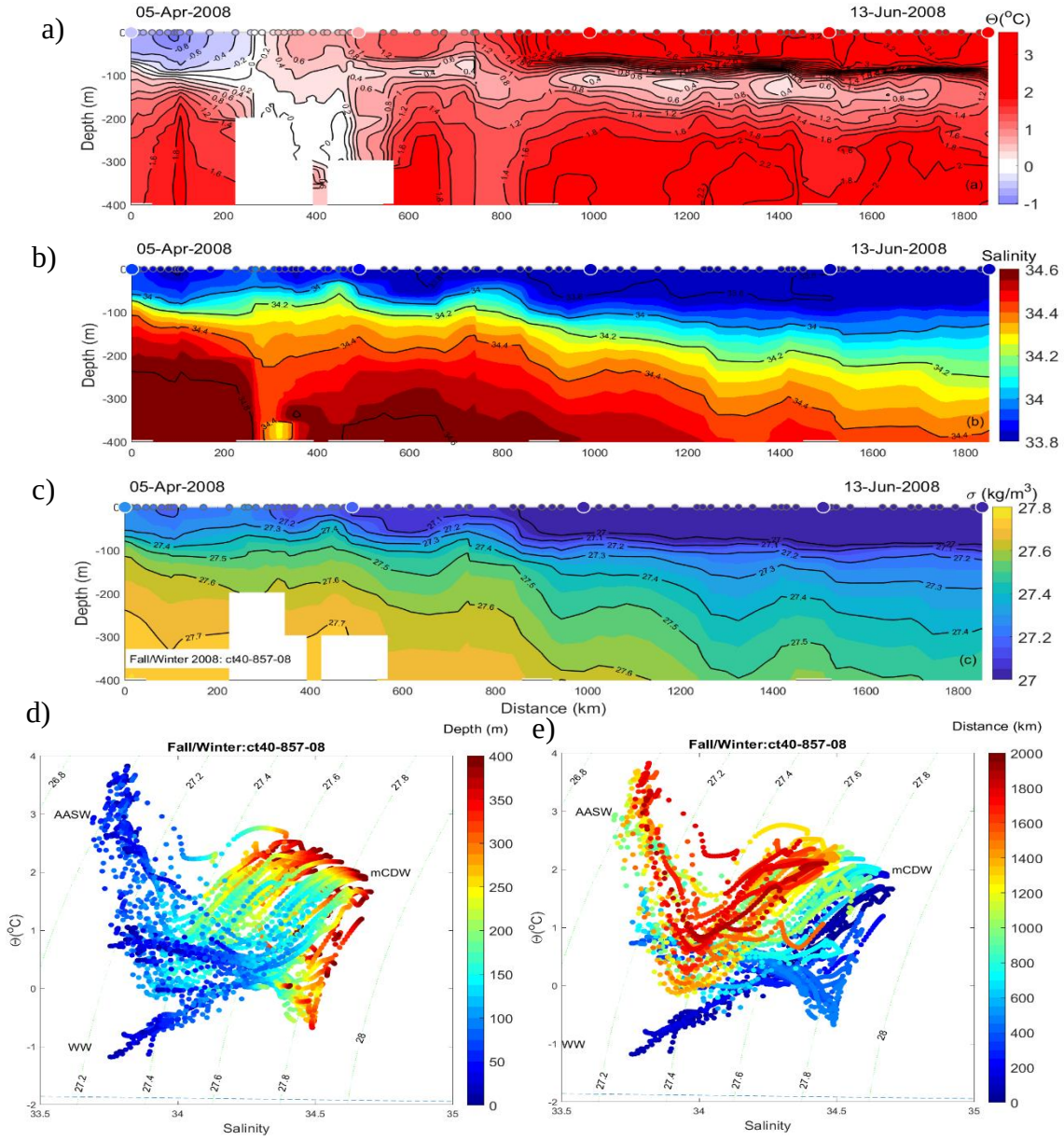

Figure 37: Fall/winter vertical sections of (a) potential temperature, (b) salinity and (c) potential density. TS diagrams with shades of colors showing (d) depth and (e) distance.)

tracks in Figure 13) though the corresponding vertical sections and TS diagram are not show in this work for brevity.

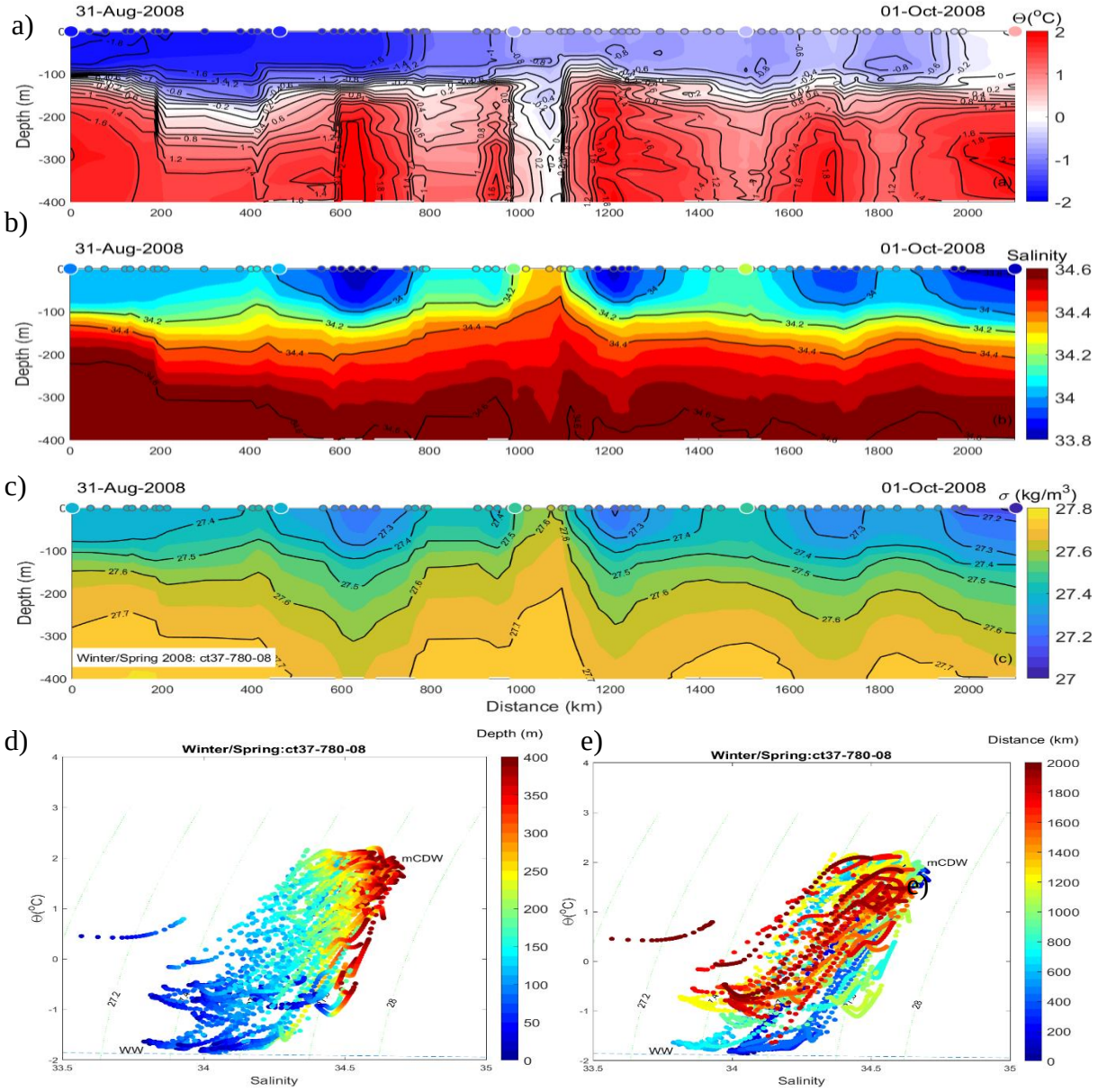

Figure 48: Winter/spring vertical sections of (a) potential temperature, (b) salinity and (c) potential density. TS diagrams with shades of colors showing (d) depth and (e) distance.

3.3.- SEASONAL WATER MASSES TRANSFORMATIONS IN THE SCOTIA SEA

On two occasions, instrumented seals were found two remained for a long period of time (from February to October/December) over a reduced area in the Scotia Sea. This allows the construction of the two TS diagrams in Figure 19, where the seasonal transformations of major water masses are successfully captured.

Starting from February (yellow shades in both panels) and evolving towards October (panel *a*; blue shades) and December (panel *b*, blue shades), the effect of the atmosphere

forcing the upper ocean is evident as the AASW signal cools from 3.4-4ºC down to near-freezing temperatures about -1.8ºC around July. By then, the subsurface minimum temperature of WW, which was evident through summer and fall, vanishes in the TS diagrams. During winter, this subsurface temperature minimum does not exist and the first 100 m of the water column are homogenously cold and around -1.8ºC due to deep convective winter mixing. Also, this wintertime branch of surface waters is saltier than its summertime counterpart due to brine rejection during sea-ice formation. From winter to spring, both panels show how the atmospheric forcing starts to warm the upper ocean again, rising the temperature from near-freezing values up to 0.6ºC (panel *a*) in October and 1.8ºC (panel *b*) in December, respectively.

At subsurface levels, the modified versions of CDW prevail, remaining in relatively warm (1ºC to 2.2ºC) and salty (34.25 to 34.6) values year-round. We attribute the broad range of CDW values here to the spatial patterns observed in previous sections, noting that both instrumented seals dived by months relatively closer to the northern and to the southern Scotia Sea. This leads to CDW having a higher (lower) influence for mixing with Weddell waters when the animals dived in the southern (northern) Scotia Sea.

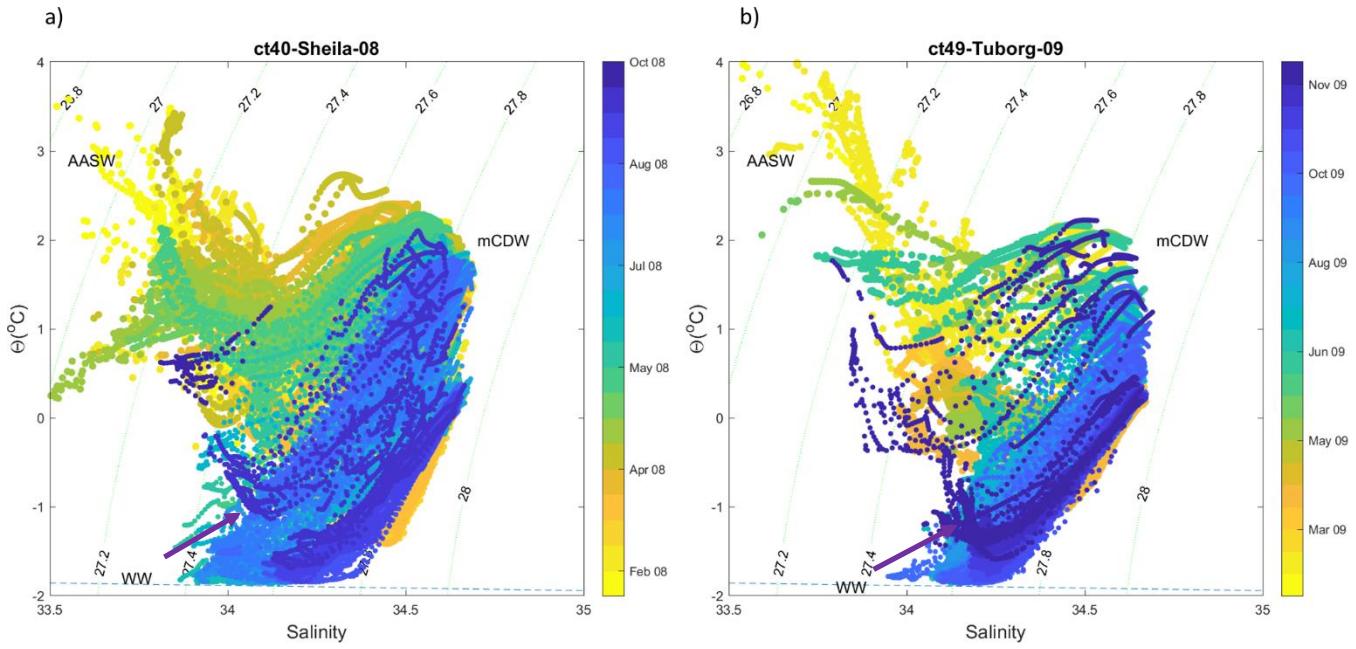

Figure 19: TS diagrams showing seasonal variations (see dates in the colorbar) for water masses measured in the Scotia Sea by the instrumented seals (a) ct40-Sheila-08; and (b) ct49-Tuborg-09.

4 DISCUSSIONS

The MEOP project represents an unprecedented database for the study of oceanographic structures which are invisible to other monitoring systems in the study area. This is due to the following two aspects, which we highlight as key.

On the one hand, instrumented seals in this region migrate every year, during the warm seasons, from the South Georgia Island and South Orkney Islands towards the south along the west Antarctic Peninsula, performing the reverse route as the colder seasons evolve. The recurrency of these routes performed by several individuals at the same time as a community allows to strengthen the robustness of observed thermohaline structures. On the other hand, seals dived indistinctively across regions deeper and shallower than 1000 m, the parking depth of Argo floats, thus enabling access to temperature and salinity observations otherwise missing due to the local hazardous weather conditions and sea-ice coverage that prevent the availability of deep-reaching ship-based measurements through the fall and winter seasons.

Furthermore, the migration routes of the seals were commonly performed in less two months over distances as long as 2000 km, reaching on occasions the sea floor but having 400 m as a generally common maximum depth for dives. This lead to the following two situations. When the migration was performed within one given season, the resulting transect allows to capture major characteristics of the upper ocean during that given season as compared to the other seasons. When the migration was performed such that two seasons occurred through it, the resulting transect allows to capture the water mass transformation of the upper ocean along unique transects where the atmospheric forcing is acting through the sampling time and space.

On occasions, seals remained diving around a nearly stationary domain in the Scotia Sea. We find these seals acted as ‘living moorings’, sampling the upper ocean over a relatively small region. This allows to record the time-varying temperature and salinity properties of local water masses through different seasons over a specific region as measured by one individual.

5 CONCLUSIONS

The results presented in this work, based on available observations from instrumented marine mammals collected by the MEOP project, lead to the following conclusions:

1.- The use of instrumented animals allows the study of ocean properties in shallow regions and seasons otherwise unreachable with traditional monitoring systems.

2.- The migration routes of the seals, which more commonly travel in groups, allows to strengthen the robustness of observed thermohaline structures given than several independent sensors (different animals) are measuring at the same time the same region.

.

6 REFERENCE

Cook, A. J., P. R. Holland, M. P. Meredith, T. Murray, A. Luckman, and D. G. Vaughan (2016),Ocean forcing of glacier retreat in the western Antarctic Peninsula, *Science*, *353*(6296), 283–286.

García, M., C. Millot, J. Font, and E. García-Ladona (1994), Surface circulation variability in the Balearic Basin, *J. Geophys. Res.*, *99*(C2), 3285–3296.

García, M. A., C. G. Castro, A. F. Ríos, M. D. Doval, G. Rosón, D. Gomis, and O. López (2002a), Water masses and distribution of physico-chemical properties in the western Bransfield Strait and Gerlache Strait during Austral summer 1995/96, *Deep-Sea Res. II*, *49*(4–5), 585–602, doi: https://doi.org/10.1016/S0967-0645(01)00113-8.

García, M. A., C. 706 G. Castro, A. F. Ríos, M. D. Doval, D. Rosón, G.and Gomis, and O. López (2002b), Physical oceanography during Hespérides cruise Fruela95, *PANGAEA*, doi: https://doi.org/10.1594/PANGAEA.825643.

García, M. A., C. G. Castro, A. F. Ríos, M. D. Doval, G. Rosón, D. Gomis, and O. López (2002c), Physical oceanography during Hespérides cruise Fruela96, *PANGAEA*, doi:https://doi.org/10.

Gordon, A. L., and B. A. Huber (1984), Thermohaline stratification below the Southern Ocean sea ice, *J. Geophys. Res.*, *89*(C1), 641–648.

Hofmann, E. E., J. M. Klinck, C. M. Lascara, and D. A. Smith (1996), *Water mass distribution and circulation west of the Antarctic Peninsula and including Bransfield Strait*, American Geophysical Union.

Klinck, J. M., E. E. Hofmann, R. C. Beardsley, B. Salihoglu, and S. Howard (2004), Water-mass properties and circulation on the west Antarctic Peninsula Continental Shelf in Austral Fall and Winter 2001, *Deep-Sea Res. II*, *51*(17-19), 1925–1946.

López, O., M. A. Garcıa, D. Gomis, P. Rojas, J. Sospedra, and A. Sánchez-Arcilla (1999), Hydro757 graphic and hydrodynamic characteristics of the eastern basin of the Bransfield Strait (Antarctica), *Deep-Sea Res. I*, *46*(10), 1755–1778.

Moffat, C., B. Owens, and R. C. Beardsley (2009), On the characteristics of Circumpolar DeepWater intrusions to the west Antarctic Peninsula continental shelf, *J. Geophys. Res.*, *114*(C5).

Orsi, A. H., T. Whitworth III, and W. D. Nowlin Jr (1995), On the meridional extent and fronts of the Antarctic Circumpolar Current, *Deep-Sea Res. I*, *42*(5), 641–673.

Park, Y.-H., E. Charriaud, and M. Fieux (1998), Thermohaline structure of the Antarctic Surface water/winter water in the Indian sector of the Southern Ocean, *J. Mar. Syst.*, *17*(1-4), 5–23.

Prézelin, B. B., E. E. Hofmann, C. Mengelt, and J. M. Klinck (2000), The linkage between Upper CircumpolarDeepWater (UCDW) and phytoplankton assemblages on thewestAntarctic Peninsula continental shelf, *J. Mar. Res.*, *58*(2), 165–202.

Sangrà, P., G. C., M. Hernández-Arencibia, A. Marrero-Díaz, A. Rodríguez-Santana, A. Stegner, A.Martínez-Marrero, J. L. Pelegrí, and T. Pichon (2011), The Bransfield current system, *Deep-Sea Res. I*, *58*(4), 390–402.

Sangrà, P., A. Stegner,M. Hernández-Arencibia, , A.Marrero-Díaz, C. Salinas, B. Aguiar-González, C. Henríquez-Pastene, and B. Mouriño-Carballido (2017), The Bransfield Gravity Current, *Deep-Sea Res. I*, *119*, 1–15.

Smith, D. A., E. E. Hofmann, J. M. Klinck, and C. M. Lascara (1999), Hydrography and circulation of the west Antarctic Peninsula continental shelf, *Deep-Sea Res. I*, *46*(6), 925–949.
Jhon D'Errico (2022). inpaint_nans (https://www.mathworks.com/matlabcentral/fileexchange/4551-inpaint_nans), MATLAB Central File Exchange. Retrieved June 30, 2022.

Patterson, S.L., & Sievers, H. A. (1980). The Weddell-Scotia Confluence, Journal of *Physical Oceanography*, *10(10)*, 1584-1610. Retrieved Jul 1, 2022, https://journals.ametsoc.org/view/journals/phoc/10/10/15200485_1980_010_1584_tws_2_0_co_2.xml Alberto C. Naveira Garabato, David P. Stevens, & Karen J. Heywood. (2003). *Water Mass Conversion, Fluxes, and Mixing in the Scotia Sea Diagnosed by an Inverse Model in: Journal of Physical Oceanography Volume 33 Issue 12 (2003)*. https://journals.ametsoc.org/view/journals/phoc/33/12/1520-0485_2003_033_2565_wmcfam_2.0.co_2.xml?tab_body=pdf.

Bizsel, K. C., & Ardelan, M. v. (2007). Weddell-Scotia Confluence Effect on the Iron Distribution in Waters Surrounding the South Shetland (Antarctic Peninsula) and South Orkney (Scotia Sea) Islands During the Austral Summer in 2007 and 2008. *Front. Mar. Sci*, *6*, 771. https://doi.org/10.3389/fmars.2019.00771.

Boehlert, G. W., Costa, D. P., Crocker, D. E., Green, P., O'brien, T., Levitus, S., And, @, & le Boeuf, B. J. (2001). *Autonomous Pinniped Environmental Samplers: Using Instrumented Animals as Oceanographic Data Collectors*.

Boehme, L., Lovell, P., Biuw, M., Roquet, F., Nicholson, J., Thorpe, S. E., Meredith, M. P., & Fedak, M. (2009). Technical Note: Animal-borne CTD-Satellite Relay Data Loggers for real-time oceanographic data collection. In *Ocean Sci* (Vol. 5). www.ocean-sci.net/5/685/2009/.

Palmer, M., Gomis, D., Flexas, M. del M., Jordà, G., Jullion, L., Tsubouchi, T., & Naveira Garabato, A. C. (2012). Water mass pathways and transports over the South Scotia Ridge west of 50°W. *Deep Sea Research Part I: Oceanographic Research Papers*, *59*, 8–24. https://doi.org/10.1016/J.DSR.2011.10.005.

R. Yu. Tarakanov. (2008). *Antarctic Bottom Water in the Scotia Sea and the Drake Passage*. https://doi.org/10.1134/S0001437009050026.

Reeve, K. A., Boebel, O., Strass, V., Kanzow, T., & Gerdes, R. (2019). Horizontal circulation and volume transports in the Weddell Gyre derived from Argo float data. *Progress in Oceanography*, *175*, 263–283. https://doi.org/10.1016/J.POCEAN.2019.04.006.

Veny, M., Aguiar-González, B., Marrero-Díaz, Á., & Rodríguez-Santana, Á. (2022). Seasonal circulation and volume transport of the Bransfield Current. *Progress in Oceanography*, *204*. https://doi.org/10.1016/j.pocean.2022.102795.

Vincent, C., Mcconnell, B. J., Ridoux, V., & Fedak, M. A. (2002). Assessment of Argos location accuracy from satellite tags deployed on captive gray seals. *Marine Mammal Science*, *18*(1), 156–166. https://doi.org/10.1111/J.1748-7692.2002.TB01025.X.

Huneke, W.G.C., Huhn, O. & Schröeder, M. Water masses in the Bransfield Strait and adjacent seas, austral summer 2013. *Polar Biol* **39,** 789–798 (2016). https://doi.org/10.1007/s00300-016-1936-8